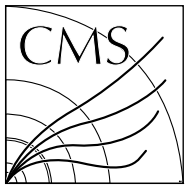

The Compact Muon Solenoid Experiment

CMS Note

Mailing address: CMS CERN, CH-1211 GENEVA 23, Switzerland

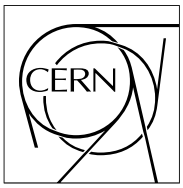

Occupancy Simulations with Stacked Pixel Layers

M. Wingham [a)], G. Hall, M. Pesaresi

Blackett Laboratory, Imperial College London, SW7 2AZ, UK

Abstract

An occupancy study is performed on a stacked pixel tracker with 200 μm thick sensors, tilted at 23° and 0.1 mm $(r-\phi)$ × 2.37 mm (z) pixels. At a luminosity of 10^{35} $cm^{-2}s^{-1}$, the occupancy of the 25 cm layer was measured through simulation to be 0.42 % ± 0.01 % (stat) ± 0.15 % (syst). This includes a scaling factor of 3 to account for the discrepancy between full and fast simulation. Occupancy increases with sensor thickness by ∼0.15 % per 100 μm. Untilting the sensors increases the occupancy by 35 % of its measured value to 0.57 %. High p_T, central tracks produce small sim-hits in both $r-\phi$ and z measuring 10^{-3} cm by 10^{-2} cm respectively. Cluster $r-\phi$ dimensions decrease with sensor thickness. Finally, for QCD jets, the center has a 20 % higher mean local occupancy than at the edge. τ-jets show a 10 % drop across the same region.

[a)] At BP, Aberdeen, UK from 07/09/09. email: mail@matthewwingham.com

1 Introduction

The upgrade to the LHC is expected to produce a $p-p$ luminosity of $10^{35}\ cm^{-2}s^{-1}$, ten times that of the current LHC design. This presents several major challenges. For example, the L1 trigger is degraded through the lack of isolated objects. Negligible improvements are seen through simply raising p_T thresholds. To reduce background rates effectively, and maintain signal efficiency, information must be included from the tracker. This solution, however, invites its own set of complications.

Incorporating information from the tracker into the L1 trigger will increase the bandwidth requirements for each bunch crossing. It will also increase the number of combinatorials for forming tracks from hits. Furthermore, the resultant track multiplicity per event is expected to increase by a factor ten, yielding similar increases in the occupancy of the detector. On-detector data reduction is essential to reduce the data volume to be transferred. This appears to be possible by correlating hits in *stacked* pixellated layers in close radial proximity [1],[2]. This approach can provide a fast way of rejecting large numbers of hits quickly. It can also provide a coarse p_T measurement for the tracks that produce such pairs of hits, or *stubs*.

Several alternative stacked tracker designs are currently being studied. The effectiveness of each design in allowing an efficient reconstruction of stubs as well as the resultant data rates are highly dependent on the detector occupancy. This note aims to provide some basic occupancy measurements made with one particular tracker design simulation that can be used as a benchmark for the tracker layout studies.

2 Detector simulation

The layout of the detector design to be studied in this note is shown by Figure 1. Four layers of standard CMS pixels, with two, three-layer endcaps, are surrounded by six stacked layers. Each stack consists of two closely spaced layers, with more coarsely pixellated sensors compared to the inner pixels. It is likely that such a large number of stacked layers will not be used in the final design. However, this arrangement allows the effect of increasing radius to be easily studied. Both pixel and stacked-pixel sensors are tilted to avoid an increased cluster size due to the Lorentz effect.

A summary of the geometry used in this note is given in Table 1. The layer radius and stacked-layer separation parameters have been chosen to optimise stub reconstruction efficiency, as described by M. Pesaresi [3]. The other parameters: thickness, tilt and dimension, are reasonable approximations based on the existing pixel subdetector. Occupancy variations with sensor thickness and tilt will also be studied in this note. Variation with pixel dimensions can be accounted for using simple scaling arguments. To be clear, a column lies along the $r-\phi$ direction, a row along z. The convention of this note will be to describe the $r-\phi$ dimension of a cluster as its *width* and the z dimension as its *length*.

As a benchmark, the main focus of this study will be on the 25 cm layer alone. As will be shown, it is simple to apply scaling arguments to extract equivalent occupancy values at higher or lower radii.

layer	radius $[cm]$	separation $[mm]$	thickness $[\mu m]$	tilt	readout-chip dimension [columns × rows]	pixel $r-\phi \times z$ $[mm \times mm]$
inner 1,2,3,4	3.9,6.8,10.9,16.0	-	285	23°	52 × 80	0.1×0.15
stacked 1,2	25,35	2	200	23°	30 × 256	0.1×2.37
stacked 3,4	55,65	2	200	13°	416 × 470	0.1×0.17
stacked 5,6	95,105	2	200	10°	416 × 957	0.1×0.17

Table 1: Breakdown of pixel barrel layers. Both inner pixel layers [4] and stacked-pixel layers are included.

To simulate the geometry described and propagate tracks through each tracking layer, CMSSW 2.2.6 [5] has been used. This allows detector simulation using GEANT4 libraries, termed *full-sim*, or a faster approach, *fast-sim*, that uses CMS specific Famos libraries. The differences between these software packages is discussed in detail in the following section.

The pixel digitisation software was configured to generate 135 electrons per ADC count. The dynamic range was 0 - 255 ADC counts or 0 - 34425 electrons. No electronic noise was simulated. $p-p$ collisions only are simulated in this study. Any pile-up quoted is a mean value - Poission fluctuations were included on an event-by-event basis.

Before any occupancy measurements from simulation are presented, the signal amplitude distribution should be understood. Figure 2 shows examples for various sensor thicknesses at 25 cm radius. The structure of each

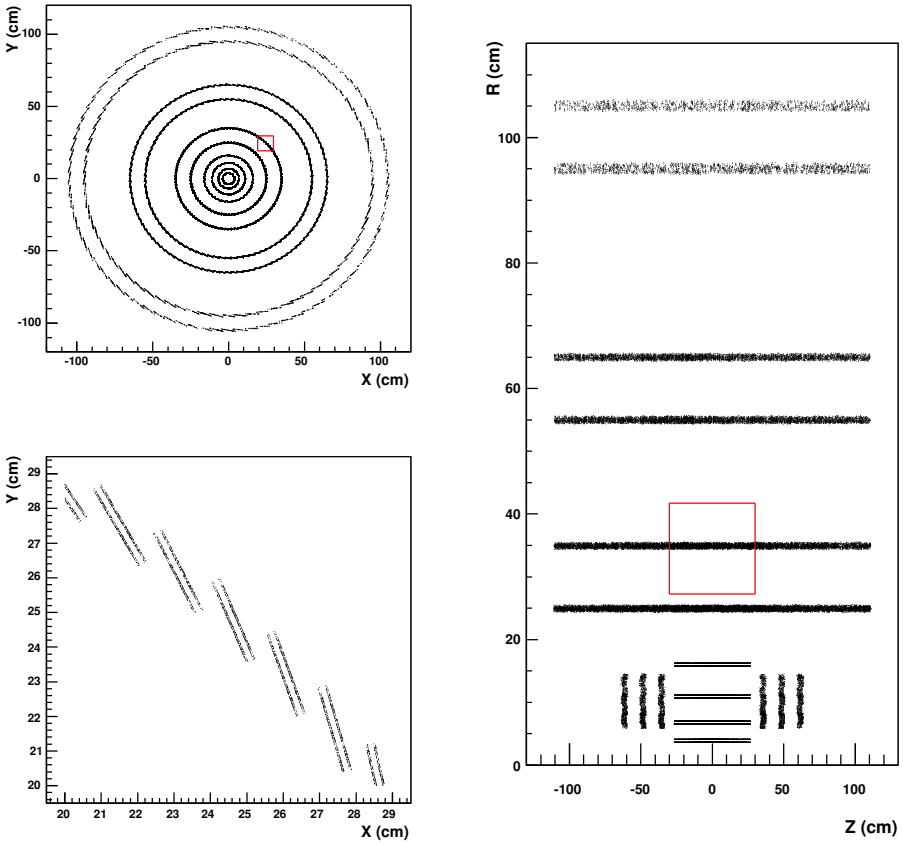

Figure 1: The inner pixels and stacked-pixel layout. Active regions are highlighted by the digitised hits recorded over 100 dimuon events with 20 events of minimum bias pile-up. Both the $x-y$ (top-left) and $r-z$ (right) planes are shown. Hits for the $x-y$ plane are recorded in the region $|z| < 30\ cm$. The $x-y$ plane close up (bottom-left) shows the region highlighted by the red boxes.

distribution is a consequence of the energy loss of all charged particles traversing the silicon in each minimum bias event. Detailed discussions of this shape can be found in [6],[7]. As expected, more energy is deposited in thicker sensors and the Landau distributions are broader.

3 Estimation from previous studies

Although no collision data are available for analysis at the time of writing, data rate and occupancy simulations have been performed for the existing pixel detector [8] and for the strip tracker [9]. The third pixel layer consists of $100 \times 150\ \mu m^2$ pixels, 11 cm from the beam pipe. An occupancy of 0.016 $\%$ was measured for the nominal LHC luminosity of $10^{34}\ cm^{-2}s^{-1}$. Correcting for layer radius and pixel dimension and scaling up by a factor of 10 for the SLHC luminosity gives an estimated occupancy of 0.5 $\%$ at 25 cm radius. Similarly, for the strip tracker, the innermost barrel layer (TIB 1) consists of 12 $cm \times 80\ \mu m$ strips 25.5 cm from the beam pipe. At the LHC design luminosity an occupancy of 2.8 $\%$ was estimated. The same scaling arguments yield an expected occupancy of 0.7 $\%$ for 100 $\mu m \times 2.5\ mm$ pixels at 25 cm radius.

These figures are very useful for cross-checking when studying the output of full and fast simulation. As will be discussed in detail in the next section, full simulation is too memory and CPU costly to run at SLHC luminosities and fast simulation makes compromises which affect the occupancy.

4 Full and Fast Simulation Occupancy Measurements

Full simulation [10],[11] of CMS is based on the GEANT4 [12] toolkit. It includes a detailed description of the materials along with the sensitive and *dead* regions, support materials, cables, cooling and electronics. Throughout

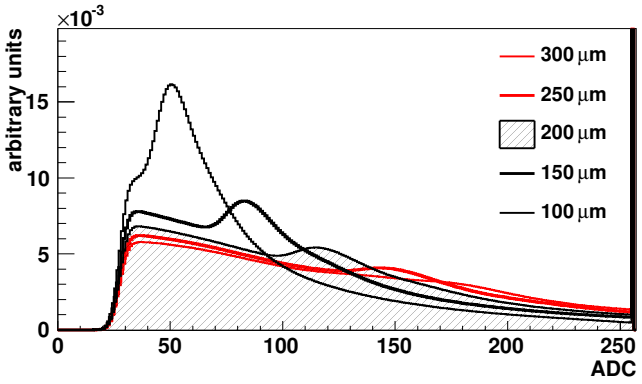

Figure 2: Stacked layer sensor signal distribution for various sensor thicknesses. Minimum bias events were used, with fast-sim and 400 events of pile-up.

the various detector volumes, the particle four-vectors are traced and the physics processes that describe a particle trajectory through matter are modeled. Results of these interactions are recorded as *sim-hits*. Particles can either be a primary four-vector generated by the Monte Carlo software or a secondary generated as a result of the GEANT4 interaction of a primary with matter.

The full simulation package used by CMSSW is configurable, allowing the various sub-detectors to be included (or not) and the magnetic field to be switched on or off. When simulating only the tracker at 4T, and with only 100 events of pile-up (corresponding to a luminosity of $2.5 \times 10^{34}\ cm^{-2}s^{-1}$, a quarter of that proposed for the SLHC) over 1000 s of CPU time were required per event. The CPU time was also measured to increase quadratically with the number of pile-up events. Furthermore, due to memory leaks, 400 events of pile-up (the full proposed SLHC luminosity) crashes at runtime. To tackle these issues and examine high luminosity conditions the more streamlined fast simulation software was required.

CMS fast-sim [13] is a CMSSW-integrated simulation tool designed to mimic the detector effects of full-sim as closely as possible without being penalised by large CPU time and memory usage. In fact, for 100 events of pile-up it has been measured to be 100 times faster than the full-sim alternative. To make this saving, a number of assumptions had to be made through dedicated parameterisations. Fast-sim exists entirely independently of the full-sim toolkit, though its accuracy is dependent on validation against it.

Figure 3 shows stacked pixel occupancy measurements against the number of pile-up events for the 25 cm layer only, as well as the variation of occupancy with layer radius when simulating 20 events of pile-up (LHC design conditions). The bottom two graphs show the full-sim/fast-sim occupancy ratio. Approximately a factor 6 discrepancy exists between the two simulation tools.

To reduce this fast-sim deficit, the package can be tuned to include certain effects which are not there by default. The minimum track p_T can be lowered from 250 MeV/c to several MeV/c and tracks that trace more than half a loop in the tracker can be included. Both of these effects can increase the CPU time and memory usage of fast-sim but not so drastically as to cause significant issues at 400 events of pile-up. Furthermore, when studying the 25 cm layer, tracks from the primary vertex can have a p_T as low as 150 MeV/c so lowering thresholds is vital to study these soft tracks effectively. From Figure 3 it can be seen that this tuning process reduces the discrepancy with full-sim to a factor 3. The occupancy ratio also remains flat with pile-up (at least up to 100 events) and layer radius. Therefore multiplying any fast-sim measurements by 3 should give a good approximation of the full-sim value. The remaining factor 2 can be explained by out-of-time pile-up and δ-rays, both of which are ignored by the fast-sim algorithms.

With the detector configuration described in Table 1, a 25 cm stacked pixel mean occupancy of 0.14 $\%$ was measured. Scaling up by a factor 3 yields a $10^{35}\ cm^{-2}s^{-1}$ luminosity full-sim projection of 0.42 $\%$. Statistical fluctuations in this figure, based on a Gaussian fit, are $\pm$ 0.01 $\%$. By far the largest uncertainties arise from various systematics, primarily from the scaling factor of 3 applied to the fast-sim measurement and the minimum bias cross section. The former is estimated to be 20 $\%$, the latter 30$\%$. Combining these values yields an 25 cm occupancy measurement of 0.42 $\%$ $\pm$ 0.01 $\%$ (stat) $\pm$ 0.15 $\%$ (syst). This figure is in approximate agreement with the estimates made in Section 3. It should be noted that all further occupancy measurements quoted in this note are generated by the tuned fast-sim package. They are therefore a factor 3 smaller than the equivalent full-sim values.

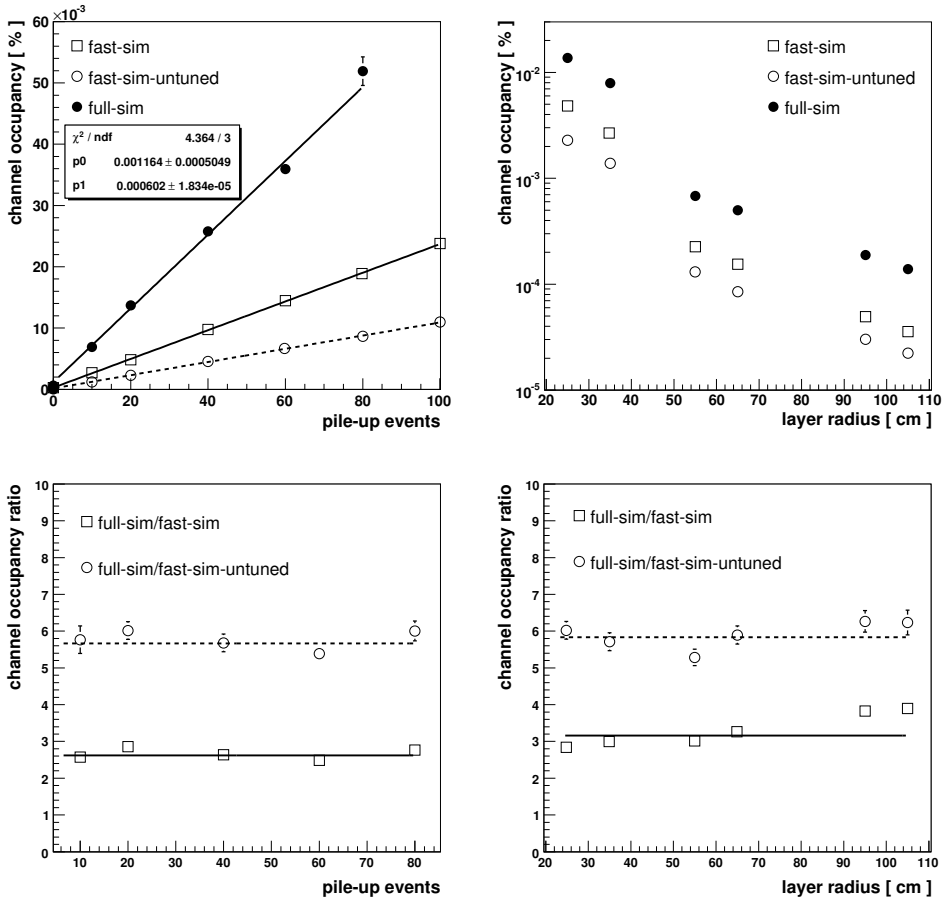

Figure 3: (top-left) 25 cm layer occupancy as a function of number of pile-up events. (top-right) Layer occupancy as a function of layer radius. Full-sim, fast-sim and *untuned* fast-sim outputs are shown for comparison. (bottom-left) Full-sim/fast-sim and full-sim/fast-sim-untuned occupancy ratios for the 25 cm stacked layer as a function of pile-up. (bottom-right) Full-sim/fast-sim and full-sim/fast-sim-untuned occupancy ratios for 20 events of pile-up as a function of stacked layer radius.

5 Occupancy variation with sensor thickness and tilt

By running at five sensor thicknesses and recording pixel occupancy of the 25 cm stacked layer, the linear trend of Figure 4 (left) was produced. Increasing the thickness from 100 μm to 300 μm serves to increase the mean occupancy by a factor of 2. As will be shown in Section 6 this is due to increasing cluster sizes in $r - \phi$ for each hit. A useful approximation is that occupancy increases by 0.05 $\%$ per 100 μm (fast-sim), corresponding to 0.15 $\%$ per 100 μm (full-sim).

Figure 4 (right) shows the occupancy measurements for the 25 cm layer for both tilted and untilted sensors. By default, sensors are tilted at the Lorentz angle to minimise cluster sizes. By untilting the sensors, the occupancy therefore increases. A tuned fast-sim occupancy increase by 35 $\%$ of its original value to 0.19 $\%$ was recorded. This would imply a full-sum untilted occupancy of 0.57 $\%$.

6 Occupancy at the level of a module column

For some stacked layer readout schemes, where hits are transferred to the periphery for comparison, the variation in the number of digis per column is important. With a mean 25 cm occupancy of 0.42 $\%$ (full-sim) at a luminosity of 10^{35} $cm^{-2}s^{-1}$, an average of 1.08 digis are expected per 256 pixel column. Figure 5 shows the variation in this number from channel-to-channel as well as the variation with pseudorapidity using the tuned fast-sim approach. There are 40 $\%$ fewer digis per column in the forward region than in the barrel center. This is because, although the number of tracks per unit of pseudorapidity increases in the forward regions, the number of columns also increases due to the cylindrical shape of the layer. This has the net effect of a reduction in column occupancy.

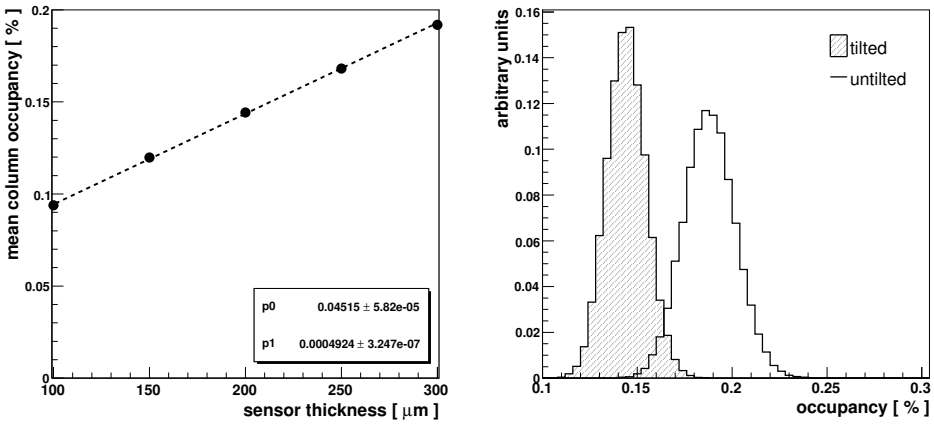

Figure 4: (left) 25 cm layer occupancy as a function of sensor thickness. (right) 25 cm layer occupancy distribution for both tilted and untilted sensors. 400 events of minimum pile-up were used with fast-sim.

The structure in the distribution, which is clearest at low $|\eta|$, is a result of the overlap of modules in z. The distribution on the right of the figure shows a sharp decrease in the number of digis per column beyond 2. Only 3.9 $\%$ of columns contain more than 2 digis, 1.8 $\%$ more than 3 digis and 0.9 $\%$ more than 4.

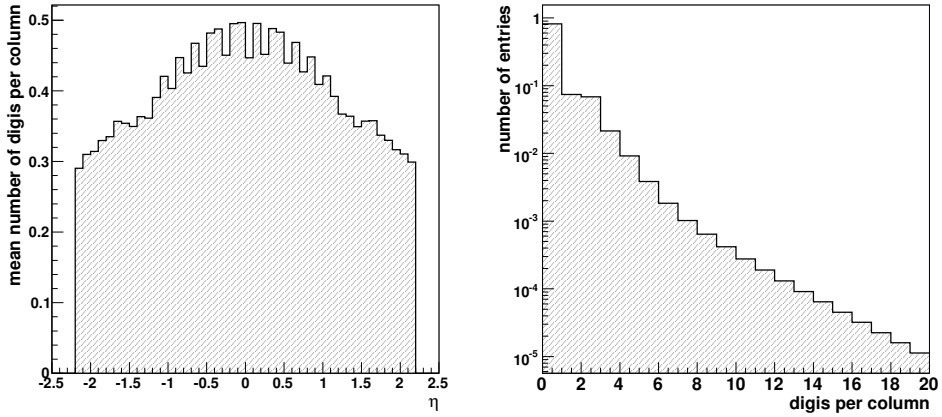

Figure 5: Number of digis per column (left) and as a function of pseudorapidity (right). Columns are 256 pixels long. Minimum bias events were used, with fast-sim and 400 events of pile-up.

Also important is the width of digi clusters in $r-\phi$, along a single column. If high p_T tracks produce wide clusters, they may be truncated in certain readout schemes. In general, clusters of neighbouring pixel digis are arranged in a 2D lattice. One particular scheme conceived by G. Hall groups the pixels along a 128-pixel column into thirty-two groups of four. Here, valid single hit patterns are defined as: 1000, 0100, 0010, 0001, 1100, 0110 and 0011. Two-hit patterns are: 1001, 1010, 0101, 1101 and 1011. Finally, rejected patterns are: 0000, 1110, 0111 and 1111. Occasionally, neighbouring fours will reject a particular cluster, for example 0001 - 1100 would reject the one and two-pixel hits as they merge into a single three-pixel hit. In this scheme, 10 bits are assigned to each group, 5 for the group location, 4 for the bit-pattern and 1 spare. Hits from neighbouring columns can then be compared to clusterize in z. Figure 6 shows the 4-bit digi pattern frequencies for minimum bias events at a $10^{35}\ cm^{-2}s^{-1}$ luminosity.

Clearly, if high p_T tracks frequently produce long strings of digis (longer than 2) then this scheme could fail (and hence require modification). Figure 7 shows $r-\phi$ cluster size distributions measured for each sensor thickness and the mean cluster width as a function of pseudorapidity. For this purpose, a cluster has been defined as a single column of neighbouring digis. Every cluster will be bordered on either side by at least one pixel with a 0 ADC readout. No gaps are permitted in a cluster.

Figure 7 (right) shows a mean cluster width (in $r-\phi$) of $\sim$1.8 pixels. This is compatible with the scheme proposed

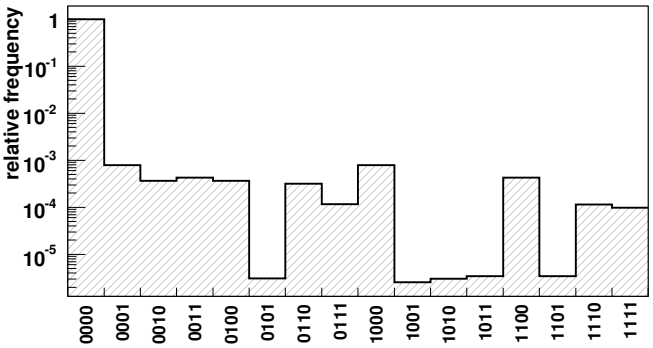

Figure 6: Pixels along each column are grouped into neighbouring fours. The digi patterns recorded are shown. For both figures minimum bias events are used with 400 events of pile-up.

above. The distribution on the left shows a small tail for three or more neighbouring pixels. In fact, for 200 μm sensors, 14.4 $\%$ of hits are 3 pixels or more in width, 5.3 $\%$ are 4 or more. Importantly, cluster widths clearly decrease with sensor thickness.

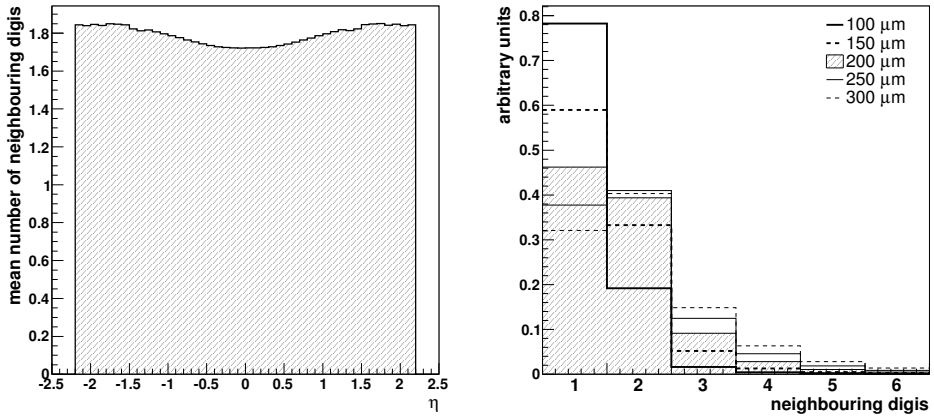

Figure 7: (left) Mean pixel cluster size in r-ϕ as a function of pseudorapidity. (right) 25 cm pixel cluster size in r-ϕ for various sensor thicknesses. For both figures, minimum bias events are used with 400 events of pile-up.

The extent of each pixel cluster in $r-\phi$ and z will be both dependent on the associated track p_T and its pseudo-rapidity. To see this dependence, the dimensions of the sim-hits associated with each charged particle trajectory have been studied. Figure 8 shows that low p_T tracks ($< 15\ GeV/c$) are wider in $r-\phi$, due to their curvature in the magnetic field. An approximate sim-hit width of $4{\times}10^{-3}\ cm$ for these tracks, compared with the $1{\times}10^{-2}\ cm$ pixel width, yields the mean number of neighbouring digis of 1.8 already discussed in this section. High p_T tracks (those of interest) are therefore much smaller in $r-\phi$. As an example, a 40 GeV track produces a sim-hit $10^{-3}\ cm$ in $r-\phi$, 10 times smaller than the pixel width in this geometry.

Sim-hits become longer in z in the forward regions due to the larger angle of incidence with the plane of the sensor. Due to the long/thin nature of pixels on the 25 cm stacked pixel layer, even the forward sim-hits with a z length of $4.5{\times}10^{-2}\ cm$ are far smaller than the 2.37mm pixel length. The vast majority of clusters on this layer are therefore only a single pixel in length.

7 Occupancy variation with jet proximity

Column occupancy distributions should also be studied as a function of ΔR from the closest jet. This will highlight any potential readout problems due to high occupancies at the center of high E_T jets. As a precursor to this study, generator-level jets have been examined. By looking at the radial distribution of charged particles within each jet, an insight into the occupancy profile can be established. Figure 9 shows the size of the cone required to contain 90 $\%$ of the charged particles; jets become more collimated with increasing E_T. Importantly, however, the curve

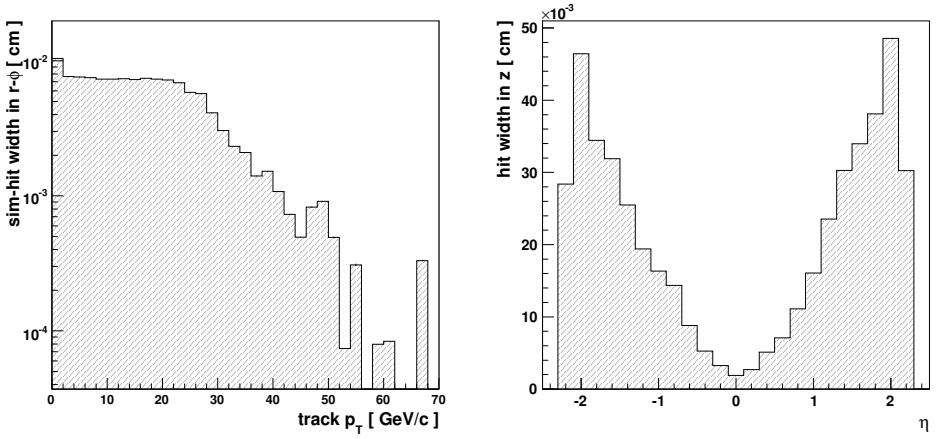

Figure 8: (left) Mean sim-hit size in $r-\phi$ as a function of associated track p_T. (right) Mean sim-hit size in z as a function of pseudorapidity. For both figures minimum bias events are used with 400 events of pile-up. Both sets of sim-hits are measured on the 25 cm stacked layer only.

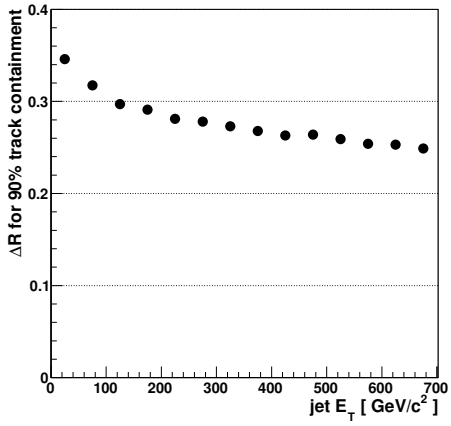

Figure 9: The mean cone size required to contain 90 $\%$ of the jets charged particles as a function of its E_T. For generator level jets without the presence of a magnetic field. A track p_T cut of 100 MeV/c has been used.

is fairly flat across a large range in transverse energy. The figure indicates that any increased local occupancy measurements would be contained within a cone size of $\sim$0.3.

Figure 10 shows the column occupancy profile for both QCD and τ- jets. Here, the number of digis in each column of the 25 cm stacked layer is recorded with respect to its distance from the center of the closest jet in ΔR. A 20 GeV E_T cut was imposed on jets. For the τ-jet study, if the closest jet to a column was not a τ-jet then the column was ignored. The position of the central pixel in each column was used. Jets were generated using a particle gun flat in E_T. Light quark flavour di-jet events were used for the QCD case, and di-τ jets in the τ case. The primary quarks/τs were restricted to the pseudorapidity region $|\eta| < 1$.

The occupancy variation from the center of a jet to its outermost edge ($\Delta R \sim 0.3$) is less than 20 $\%$ for QCD jets and 10 $\%$ for τ-jets. Taking the full-sim mean occupancy of 0.42 $\%$, a 20 $\%$ increase would imply a peak local occupancy of 0.5 $\%$. This should still be of no great concern to the example readout scheme described above. Finally, it should be noted that the variation across jet E_T bins is minimal. Higher E_T jets are slightly more collimated, which is to be expected, but the occupancy spike at the jet center does not increase sharply with jet E_T.

After digi clusterization, the next level of reconstruction of the stacked pixel detector will be the generation of stubs. Stubs are the correlated pairs of hits that exist on neighbouring stacked layers. Stubs can also be generated from unclusterised digis which is the case in this note. Associations are made based on windows in $r-\phi$ and z location. Figure 11 is analogous to Figure 10, but shows the number of stubs per module rather than the mean column occupancy. The profile is more exaggerated for the stubs case i.e. the peak is much sharper at the jet

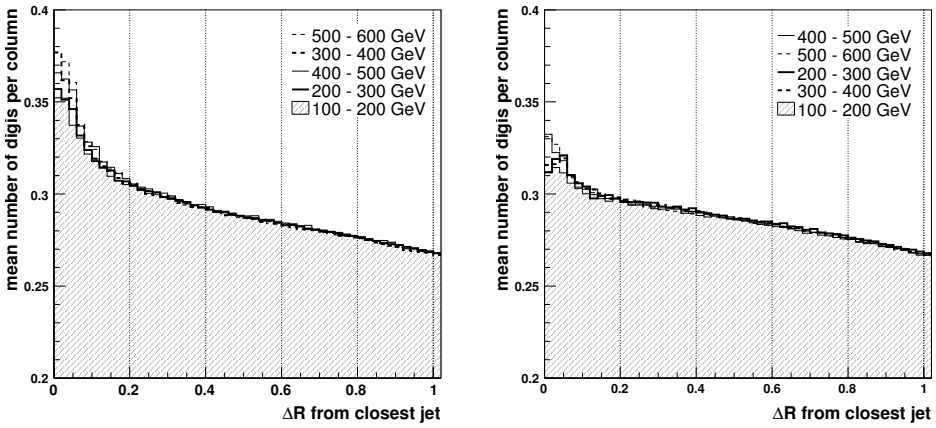

Figure 10: Number of digis per column as a function of the separation, ΔR, between the column and its closest QCD-jet (left) and τ-jet (right). Various jet E_T bins are shown.

center which shows the effectiveness of generating digi stubs to select high E_T QCD and τ - jets. Similarly for the column occupancy profile, stub populations are more collimated for higher E_T jets.

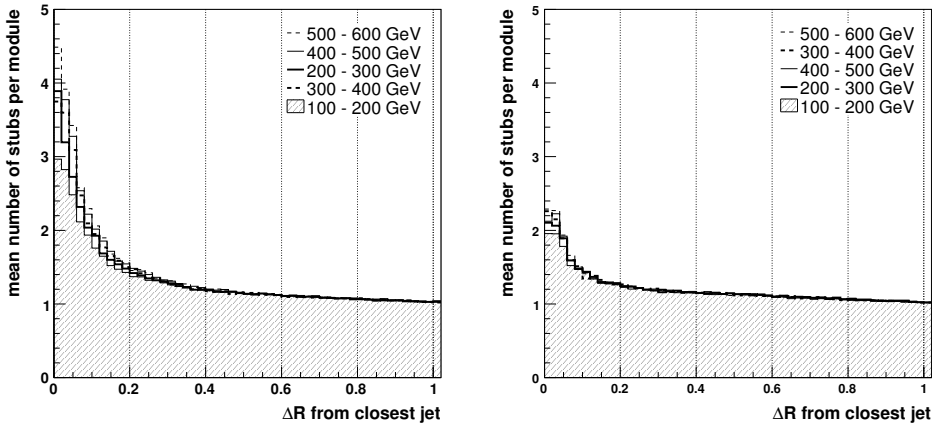

Figure 11: The number of pixel stubs per module as a function of the separation, ΔR, between the column and its closest QCD-jet (left) and τ-jet (right). Various jet E_T bins are shown.

8 Summary

One possible way of introducing tracking information into the L1 trigger at a $p-p$ luminosity of $10^{35}\ cm^{-2}s^{-1}$ would be to use one or more stacked layers of pixels surrounding the existing inner CMS pixel detector. This would provide coarse p_T information on hard tracks through the correlation of pairs of hits called *stubs*. This study aimed to estimate the occupancy of such a sub-detector using simulation. Previous simulation estimates made using the existing CMS pixel 11 cm layer and microstrip TIB layer 1 were scaled to provide an estimate for the proposed stacked tracker 25 cm layer. Values of 0.5 $\%$ and 0.7 $\%$ respectively were calculated.

Due to CPU time constraints and memory leaks, CMS full-sim cannot be run at a $10^{35}\ cm^{-2}s^{-1}$ luminosity (400 events of pile-up). Full-sim and fast-sim were run in parallel to a maximum of $2\times10^{34}\ cm^{-2}s^{-1}$ (80 events of pile-up) for comparison. A fixed factor 6 discrepancy was measured at all pile-ups and layer radii from 20 cm to 105 cm. By tuning the fast-sim algorithms to include tracks with a p_T lower than 250 MeV/c and loopers, the discrepancy reduces to a factor 3. By measuring the tuned fast-sim occupancy at $10^{35}\ cm^{-2}s^{-1}$ and scaling by this factor 3 to account for the fast sim discrepancy a 25 cm occupancy measurement of 0.42 $\% \pm 0.01\ \%$ (stat) $\pm$ 0.15 $\%$ (syst) is made. Here, the systematic errors are estimated from minimum bias cross section uncertainties and the error in the full-sim/fast-sim scaling factor.

Occupancy variation with sensor thickness and tilt was also computed. Occupancy increases linearly with thickness, doubling from 100 μm to 300 μm, corresponding to an increase by $\sim$0.15 $\%$ per 100 μm. This is due to increasing cluster sizes in $r - \phi$ with each hit. Reducing the tilt from 23° to 0° also increases cluster width by 35 $\%$ due to the Lorentz effect.

Occupancy at the level of a module column should also be understood for the purpose of on-detector readout schemes. A 256 pixel column will contain an average of 1.08 digis. Also important is the $r - \phi$ cluster width distribution. For 200 μm thick sensors, 14.4 $\%$ of hits are 3 pixels or more in width and 5.3 $\%$ are 4 or more. Cluster widths decrease with sensor thickness. High p_T, central tracks produce small sim-hits in both $r - \phi$ and z measuring 10^{-3} cm by 10^{-2} cm respectively.

Finally, column occupancy has been studied as a function of jet proximity. For QCD jets, the center has a 20 $\%$ higher mean column occupancy that at the edge. τ-jets show a 10 $\%$ drop across the same range. The same profiles shown for stub occupancies highlights their usefulness in selecting high E_T jets.

References

[1] H. W. K. Cheung et al. "Pixel Group Preparatory Workshop on Future Upgrades: Report from Working Group 3 - Level 1 Tracking Triggers using the Pixel Detector" CMS IN 2007/011

[2] J. A. Jones "Development of trigger and control systems for CMS" CERN-THESIS-2007-041

[3] M. Pesaresi "CMS L1 Track Trigger Simulation" $http://indico.cern.ch/contributionDisplay.py?contribId=19\&confId=47853$

[4] C. Amsler et al. "Mechanical Design and Material Budget of the CMS Barrel Pixel Detector" CMS NOTE 2009/006

[5] $http://twiki.cern.ch/twiki/bin/view/CMS/WorkBook$

[6] A. Giammanco "Particle Identification with Energy Loss in the CMS Silicon strip Tracker" CMS AN 2007/008

[7] K. Krajczar and G. I. Veres "Pseudorapidity distributions of charged hadrons in minimum bias p-p collisions at sqrt(s) = 14 TeV" CMS AN 2008/018

[8] D. Kotlinski, "Pixel Detector Data Rates and Inefficiencies", CMS IN 2003/004.

[9] O. Kodolova et al., "Expected Data Rates from the Silicon Strip Tracker", CMS NOTE 2002/047.

[10] V. Daniel Elvira et al., "Readiness of the CMS Detector Simulation", IEEE 2007.

[11] S. Banerjee, "Readiness of the CMS Simulation towards LHC startup", CMS CR 2007/000.

[12] $http://geant4.cern.ch$

[13] $https://twiki.cern.ch/twiki/bin/view/CMS/SWGuideFastSimulation$